

# The influence of small scale magnetic field on the polar cap X-ray luminosity of old radio pulsars

**D. P. Barsukov**

Ioffe Physical-Technical Institute of the Russian Academy of Sciences, Saint-Petersburg,  
Russian Federation  
Saint-Petersburg State Polytechnical University, Saint-Petersburg, Russian Federation

**O. A. Goglichidze and A. I. Tsygan**

Ioffe Physical-Technical Institute of the Russian Academy of Sciences, Saint-Petersburg,  
Russian Federation

E-mail: [tsygan.astro@mail.ioffe.ru](mailto:tsygan.astro@mail.ioffe.ru)

**Abstract.** The influence of small-scale magnetic field on the polar cap heating by returning positrons is considered. The returning positron current is calculated in the framework of two models of rapid and gradual screening. To calculate the electron-positron pair production rate we take into account only the curvature radiation of primary electrons and its absorption in magnetic field. We use the polar cap model with steady space charge limited electron flow. It is shown that the rapid screening model is in the better agreement with observations of old (age  $> 10^6$  years) radio pulsars. The gradual screening model usually leads to too strong heating and too large X-ray luminosities.

## 1. Introduction

The problem of magnitude of the returning positron current which flows through inner gaps and causes the polar cap heating has not been yet definitely solved. Here we present the comparison of two models of returning current calculation for old isolated normal radio pulsars with characteristic age  $\tau = P/(2\dot{P}) \geq 10^6$  years. We assume that pulsar magnetosphere can be described by Goldreich-Julian model [1]. We assume that the inner gaps occupy entire pulsar tube cross-section and neglect the input of outer gaps. Also we assume that inner gaps are stationary and operate in regime of space charge limited flow with electron emission from star surface.

## 2. The small-scale magnetic field

Let the neutron star have a radius  $r_{ns}$  and dipolar magnetic moment  $\vec{m}$  (its field at magnetic pole is  $B_{dip} = 2m/r_{ns}^3$ ). We assume also that a small-scale magnetic field with strength  $B_{sc}$  and characteristic scale  $\ell \approx r_{ns}/10$  presents nearby the polar cap. For simplicity we suppose that  $\vec{B}_{sc}$  is parallel to surface (and  $\vec{B}_{sc} \cdot \vec{m} = 0$ ) and denote by  $\psi$  ( $0 \leq \psi \leq \pi$ ) the angle between  $\vec{B}_{sc}$  and plane containing  $\vec{\Omega}$  and  $\vec{m}$  (see Fig. 1). We describe this component by additional magnetic



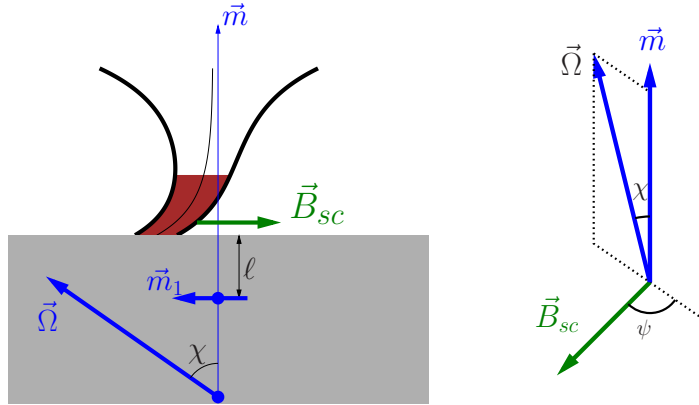


**Figure 1.** The orientation of small-scale magnetic field  $\vec{B}_{sc}$ .

moment  $\vec{m}_1$  located in the polar region of the neutron star at depth  $\ell$  [2]:

$$\vec{B} = \frac{3\vec{r}(\vec{r} \cdot \vec{m}) - \vec{m}r^2}{r^5} + \frac{3\vec{\rho}(\vec{\rho} \cdot \vec{m}_1) - \vec{m}_1\rho^2}{\rho^5}, \quad (1)$$

where  $\vec{\rho} = \vec{r} - (r_{ns} - \ell)\vec{e}_z$ ,  $\vec{m} = m\vec{e}_z$ .

In the reference frame rotating with the star all quantities do not depend on time, so we can write

$$\Delta\Phi = -4\pi(\rho - \rho_{GJ}), \quad \vec{E} = -\vec{\nabla}\Phi, \quad (2)$$

where  $\rho_{GJ} = \frac{\Omega B}{2\pi c}\tilde{\rho}_{GJ}$  is Goldreich-Julian density [1],  $\rho = \frac{\Omega B}{2\pi c}\tilde{\rho}$  and  $B$  is magnetic field strength. It is worth to note that without frame dragging  $\tilde{\rho}_{GJ}(z) \approx -\cos\tilde{\chi}$ , where  $\tilde{\chi}$  is the angle between  $\vec{B}$  and  $\vec{\Omega}$ . We choose  $\Phi = 0$  at surface and pulsar tube boundaries and take into account free electron emission condition  $E_{||}|_{z=0} = 0$  [3], where  $E_{||} = (\vec{B} \cdot \vec{E})/B$  and  $z$  is the altitude above star surface. We assume that the particles inside the pulsar tube move along field lines  $\vec{v} \parallel \vec{B}$  with relativistic velocity  $v \approx c$ , so continuity equation  $\text{div}(\rho\vec{v}) = 0$  may be rewritten as  $(\vec{B} \cdot \vec{\nabla})\tilde{\rho} = 0$  and, hence,  $\tilde{\rho}$  is constant along field lines.

### 3. Rapid screening model

The rapid screening model was proposed in [3]. According to this model pulsar tube is divided into three parts (see Fig. 2):

- 1)  $0 < z < z_c$  acceleration region (pulsar diode)

There is no pair production and no pair-plasma to screen the electric field. Thus, a large parallel electric field  $E_{||}$  is present here which accelerates the electrons. The accelerated electrons, moving along curved field lines, radiate curvature gamma photons. The latter photons after some propagation are converted into electron-positron pairs. This determines the upper boundary  $z = z_c$  of this region. The altitude  $z = z_c$  is practically equal to the altitude of pair formation front [4].

- 2)  $z_c < z < z_r$  partial screening region

There is pair production but the pairs do not have time to screen electric field completely. So, small electric field  $E_{||}$  is present here which decelerates positrons. Some of them change the velocity sign and begin to move downwards, forming the returning positron current.

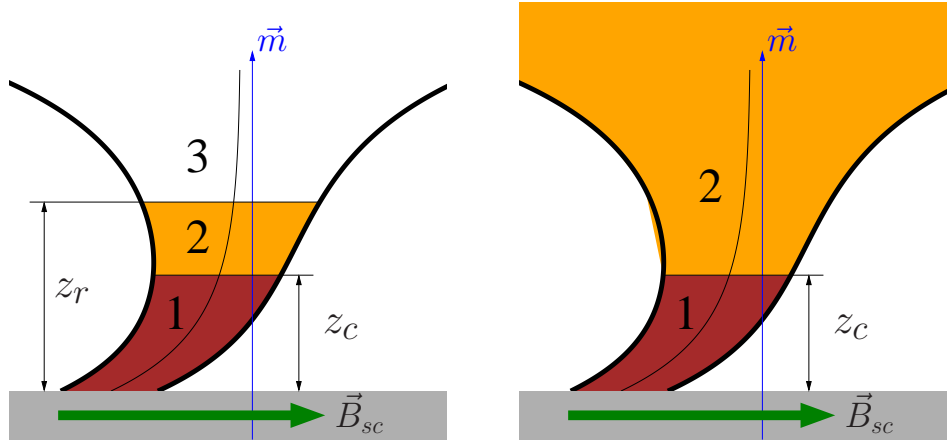


**Figure 2.** A schematic view of pulsar tube in the framework of rapid screening model (left panel) and gradual screening model (right panel). Different regions are marked as follows: 1 – the acceleration region (diode), 2 – the partial screening zone, 3 – the full screening zone.

These positrons return back into pulsar diode, become accelerated by the large electric field and hit the star's surface.

This leads to polar cap heating.

### 3) $z > z_r$ full screening region

This region is filled by large amount of electron-positron pairs, which totally screen the electric field. In [3] it was assumed that  $E_{||} = 0$  in this region. And, hence, the positrons do not decelerate and change the velocity sign here. Consequently, this region does not give an input into returning positron current.

To determine the altitude  $z_r$  the following conditions were proposed in [3]

$$E_{||}|_{z=z_r} = 0 \quad \text{and} \quad (\vec{B} \cdot \vec{\nabla})E_{||}|_{z=z_r} = 0. \quad (3)$$

The first condition means that the electric field is continuous at  $z = z_r$ , the second means that at  $z = z_r$  the charge density is continuous too. If electron-positron pairs are mainly generated by curvature radiation photons absorption in magnetic field, the energy of positrons is relatively small  $\sim 10^2 - 10^4$  MeV and its number increases very rapidly with the altitude. Hence, the length of partial-screening region is small  $z_r - z_c \ll z_c, \ell$  [4]. So, assuming that the pulsar tube is thin  $r_t \ll \ell$ , where  $r_t$  is the pulsar tube radius, it is possible to estimate returning positron density flowing along central open field line as

$$\tilde{\rho}_{ret} \approx -r_t \left. \frac{\partial \tilde{\rho}_{GJ}}{\partial z} \right|_{z=z_c} F\left(\frac{z_c}{r_t}\right), \quad (4)$$

where function  $F(x)$  may be approximated as  $F(x) \approx \frac{4x}{16+15x} \left(1 + 1.19 \frac{x}{1+x^2}\right)$  and  $F(x) \approx \frac{x}{4}$  for  $x \ll 1$ ,  $F(x) \approx \frac{4}{15}$  for  $x \gg 1$ .

## 4. Gradually screening model

Harding and Muslimov have shown [4] that if we accept the assumptions that

- 1) all quantities do not depend on time  $t$  (stationary case)

- 2) pairs are affected only by the mean electric field
- 3)  $\tilde{\rho}_{GJ}$  monotonically decreases with altitude  $z$

then the conditions (3) can not be satisfied at the same point. So, there is no stationary solution. To solve this problem they proposed that the full screening region does not exist, and pulsar tube consists of two parts: 1) acceleration region and 2) partially screening region (see Fig. 2). Hence, the electric field which decelerates positrons exists everywhere. In [4] it is assumed that for  $z > z_c$  electric field falls exponentially and very quickly becomes negligibly small and, consequently, it does not cause large positron deceleration. Therefore, Ref. [4] proposed to replace (3) by the condition

$$\Phi \rightarrow \text{const. at } z \rightarrow +\infty. \quad (5)$$

But if the electric field (very small, of course) penetrates deep into plasma, all altitudes above  $z_c$  give an input into returning current [5]. Potential  $\Phi$  does not change significantly along the field lines at  $z \geq z_c$  and positrons are reversed to support  $\tilde{\rho} - \tilde{\rho}_{GJ} \approx \text{const.}$  along the field lines at  $z \geq z_c$ . Hence, the value of the returning positron current formed at  $z_c \leq z \leq z_f$  may be estimated as

$$\tilde{\rho}_{ret} \approx -\frac{1}{2}(\tilde{\rho}_{GJ}(z_f) - \tilde{\rho}_{GJ}(z_c))$$

We suppose that  $z_f \approx (3 \div 15)r_{ns}$  is a good choice. This choice satisfies two conditions:

- (i)  $z_f < z_{rad}$ , where  $z_{rad} \approx (5 \div 50)r_{ns}$  is the altitude at which plasma waves begin to affect the pair-dynamics, so that the assumption 2) becomes invalid. Hence, at  $z \geq z_{rad}$  it is possible to satisfy both conditions (3).
- (ii)  $z_f < z_{max}$ , where  $z_{max} \approx (1 \div 5)r_{ns}$  is the altitude at which the function  $\tilde{\rho}_{GJ}$  has a minimum. It is easy to show that there exists a solution satisfying the both conditions (3) at  $z_r \approx z_{max}$ .

Also it is worth noting that  $\tilde{\rho}_{GJ}$  does not change significantly at those altitudes, so any  $z_f$  value from the selected range may be appropriate.

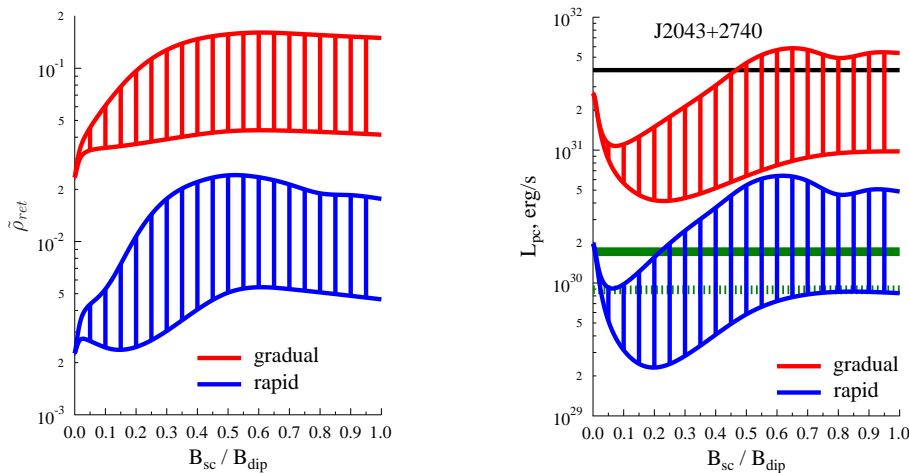


**Figure 3.** The left panel shows the returning positron current calculated in the framework of two models for pulsar J2043+2740,  $B_{dip} = 7.1 \cdot 10^{11}$  G,  $P = 96$  ms,  $\tau = 1.2 \cdot 10^6$  years,  $\chi = 55^\circ$ . The corresponding polar cap luminosity is shown in right panel. Upper limits of polar cap emission from [9] are shown by green lines, solid when we see one cap, dashed when we see both caps. The emission from the stellar surface is taken from [10] and is shown by black line.

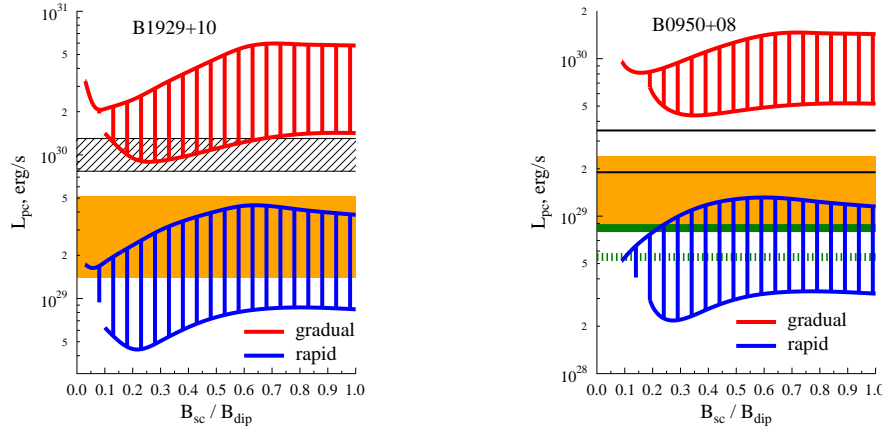


**Figure 4.** The polar cap luminosity  $L_{pc}$  for B1929+10 is shown in the left panel,  $B_{dip} = 1.0 \cdot 10^{12}$  G,  $P = 0.23$  s,  $\tau = 3 \cdot 10^6$  years,  $\chi = 45^\circ$ . The luminosity  $L_{pc}$ , which is taken from [12], is shown by orange area. The  $L_{pc}$  luminosity range from [13] is shown by black dashed area. The polar cap luminosity  $L_{pc}$  for B0950+08 is shown in right panel,  $B_{dip} = 4.9 \cdot 10^{11}$  G,  $P = 0.25$  s,  $\tau = 17.5 \cdot 10^6$  years,  $\chi = 30^\circ$ . The luminosities  $L_{pc}$  from [10] are shown by orange area and black lines. The upper limits from [9] are shown by green lines, solid when we see one cap, dashed when we see both caps.

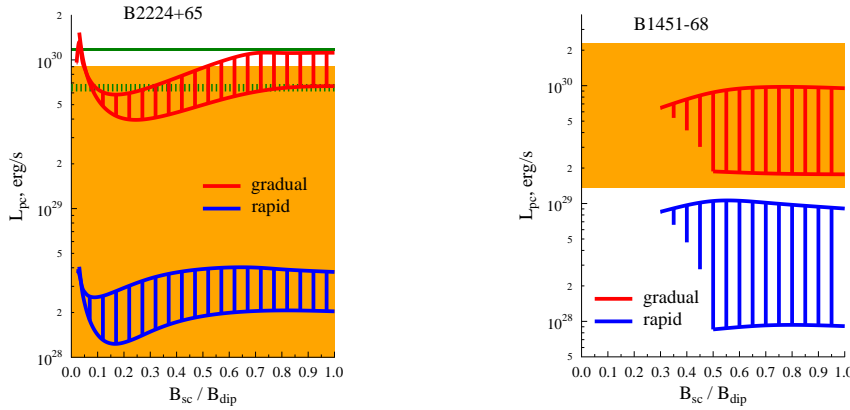


**Figure 5.** The polar cap luminosity  $L_{pc}$  for B2224+65 is shown in left panel,  $B_{dip} = 5.2 \cdot 10^{12}$  G,  $P = 0.68$  s,  $\tau = 1.1 \cdot 10^6$  years,  $\chi = 16^\circ$ .  $L_{pc}$  from [14] is shown by solid green line. Upper limit from [15] is shown by dashed green line, upper limit from [10] is shown by orange area. The polar cap luminosity  $L_{pc}$  for B1451-68 is shown in right panel,  $B_{dip} = 3.2 \cdot 10^{11}$  G,  $P = 0.26$  s,  $\tau = 42.5 \cdot 10^6$  years,  $\chi = 50^\circ$ . The luminosities  $L_{pc}$  taken from [16] are shown by orange area.

## 5. Results

The polar cap luminosity  $L_{pc}$  is estimated as

$$L_{pc} = \int e\Phi|_{z=z_c} \frac{\Omega B}{2\pi c e} \bigg|_{z=0} \tilde{\rho}_{ret} dS.$$

The results of calculation for J2043+2740, B1929+10, B0950+08, B2224+65 and B1451-68 pulsars for  $B_{sc} \leq B_{dip}$  and  $0 \leq \psi \leq \frac{\pi}{2}$  are shown in Figs. 3–5. The pulsars parameters are taken from [6] and the inclination angles  $\chi$  from [7, 8]. The possible values  $L_{pc}$  calculated in the

framework of rapid screening model are shown by blue region and calculated in the framework of gradual screening model is shown by red region. In both cases, lower boundaries of the regions correspond to  $\psi = \frac{\pi}{2}$  and upper boundaries to  $\psi = 0$ . For J2043+2740, B1929+10 and B0950+08 gradual screening model predicts luminosities exceeding the observed values. However, for B2224+65 and B1451-68 pulsars gradual screening model may be more appropriate.

## 6. Discussion

The disagreement between the prediction of gradual screening model and observations may be explained in several ways. The most obvious explanation is the existence of large surface magnetic field  $B_{surf} > 10^{14}$  G. In this case, there is no free charge emission and instead of steady charge limited flow model the model of vacuum gap must be used [17]. The disagreement may be explained by large redshift which we do not take into account at all. However this means that  $r_{ns} < 2r_g$ , where  $r_g$  is gravitational radius of star.

The disagreement can also arise due to some viscous force acting on secondary particles [18]. This force may be related to backflowing radiation [19, 20, 21], the radiation closed inside the diode [22, 23] or the radiation coming from deep layers of neutron star [24].

## Acknowledgments

The work has been supported by the RFBR (project 13-02-00112), by the State Program “Leading Scientific Schools of the Russian Federation” (grant NSh-4035.2012.2) and by the Ministry of Education and Science of Russian Federation (agreement No.8409).

## References

- [1] Beskin V S, Gurevich A V and Istomin Ya N *Physics of The Pulsar Magnetosphere* (Cambridge University Press, 1993)
- [2] Gil J A, Melikidze G I and Mitra D 2002 *A&A* **388** 235
- [3] Arons J, Fawley W M and Scharlemann E T 1979 *ApJ* **231** 854
- [4] Harding A K and Muslimov A G 2001 *ApJ* **556** 987
- [5] Lyubarskii Yu E 1992 *A&A* **261** 544
- [6] Manchester R N, Hobbs G B, Teoh A and Hobbs M 2005 *Astron. J.* **129** 1993 (*Preprint astro-ph/0412641*)  
<http://www.atnf.csiro.au/research/pulsar/psrcat>
- [7] Rankin J M 1993 *ApJSS* **85** 146
- [8] Malov I F and Nikitina E B 2011 *Astron. Rep.* **55** 19
- [9] Becker W, Weisskopf M C, Tennant A F, Jessner A, Dyks J, Harding A K and Zhang Shuang N 2004 *ApJ* **615** 908
- [10] Zavlin V E and Pavlov G G 2004 *ApJ* **616** 452
- [11] Noutsos A et al. 2011 *ApJ* **728** 77
- [12] Misanovic Z, Pavlov G G and Garmire G P 2008 *ApJ* **685** 1129
- [13] Gil J, Haberl F, Melikidze G, Geppert U, Zhang B and Melikidze G Jr 2008 *ApJ* **686** 497
- [14] Hui C Y, Huang R H H, Trepl L, Tetzlaff N, Takata J, Wu E M H and Cheng K S 2012 *ApJ* **747** 74
- [15] Hui C Y and Becker W 2007 *A&A* **467** 1209
- [16] Posselt B, Pavlov G G, Manchester R N, Kargaltsev O and Garmire G P 2012 *ApJ* **749** id 146
- [17] Gil J, Melikidze G I and Geppert U 2003 *A&A* **407** 315
- [18] Shibata S, Miyazaki J and Takahara F 1998 *MNRAS* **295** L53
- [19] Melikidze G and Gil J 2006 *Chin. J. Astron. Astrophys.* **6** Suppl. 2, 81
- [20] Dyks J, Frackowiak M, Slowikowska A, Rudak B and Zhang Bing 2006 *Chin. J. Astron. Astrophys.* **6** Suppl. 2, 85
- [21] Lomiashvili D, Machabeli G and Malov I 2007 Drift Wave Model of Rotating Radio Transients *Preprint astro-ph/0709.2019*
- [22] Kontorovich V M and Flanchik A B 2007 *JETP Letters* **85** 267
- [23] Kontorovich V M and Flanchik A B 2013 *Astrophysics and Space Science* **345** 169
- [24] Sedrakian D M, Harutyunyan A S and Hayrapetyan M V 2013 *Astrophysics* **56** 229